

Pore Size Control in Cross-Linked Polymer Resins by Reverse Micellar Imprinting

X. X. Zhu,* K. Banana, and R. Yen

Département de chimie, Université de Montréal, C.P. 6128, succursale Centre-ville, Montréal, Québec H3C 3J7, Canada

Received October 23, 1996; Revised Manuscript Received February 7, 1997[®]

ABSTRACT: We have synthesized highly cross-linked porous polymer resins with controlled pore sizes using the template imprinting technique. The polymer resins were prepared by dissolving reverse micelles in a mixture of monomers and cross-linkers followed by bulk polymerization initiated with a free radical initiator and UV irradiation. Styrene and divinylbenzene were used for the polymer matrix, and sodium bis(2-ethylhexyl) sulfosuccinate (AOT) was used as the surfactant for the formation of reverse micelles. The size of the cavities inside the polymer resins was controlled by adjusting the water content in the reverse micelles prior to polymerization. The surface area, pore volume, and pore size of the polymers were determined by gas adsorption experiments. The average diameter of the pores in the polymers was found to be proportional to the water content in the micelles, hence the micellar size. The surface area and total pore volume are also influenced by the micelle/cavity size. The pore size distribution in the polymers also depends on the size of reverse micelles. With lower water content in the reverse micelles, the size of the cavities in the polymer resins is smaller and more uniform.

Introduction

Porous polymer resins with a certain predefined pore size can be useful in many applications, such as selective catalysis of a chemical reaction, separation of compounds closely related in structure and properties, and adsorption and exchange of specific anions or cations. The principle of size exclusion has long been used in the fractionation of macromolecules of different molecular weights. It has also been demonstrated that polymers with size specificity can be used in chemical catalysis.¹ The study of the diffusion of solvent and solute molecules in polymer systems confirmed the marked effect of molecular size and shape of the diffusant molecules.^{2,3} Indeed, the size and shape of the molecules or molecular aggregates can play important roles in the chemical processes.^{4,5} The desired size and shape specificity can be achieved by the template imprinting techniques.^{6–8} During the preparation of the polymers, molecular templates with well-defined size and shape are mixed with the monomers and cross-linking agents. Once the polymerization is completed, these templates can be removed by a simple extraction or a combined chemical hydrolysis and extraction so that the polymer is left with imprints of the original templates. These polymers can be regarded as solid enzymes with molecular recognition abilities. Molecularly imprinted polymers have already found applications in the separation of isomers and enantiomers,⁹ protein purification,^{10,11} trace adsorption and drug assays,¹² and stereoselective synthesis.¹³

Some of the reverse micelles can solubilize large amounts of water, especially the micelles formed by sodium bis(2-ethylhexyl) sulfosuccinate (a surfactant commonly known as Aerosol OT or AOT), which can attain a water-to-AOT molar ratio (*W*) of well beyond 20 in nonpolar organic solvents.^{14,15} Depending on the amount of water solubilized in the micelles, the sizes of the water droplets are different and the water encased in the droplets has a higher acidity and is less mobile than bulk water.^{16,17} Porous polymers based on styrene

and methyl methacrylate have been prepared by the use of water-in-oil microemulsions.^{18,19} Pioneer work on the polymerization of styrene–divinylbenzene solutions of AOT reverse micelles containing copper cations was reported by Menger *et al.*,^{20,21} who explored the use of such materials as catalysts in the hydrolysis of phosphate ester and as chromatographic packing materials. There have also been reports on the preparation of similar cross-linked polymers possessing positively-charged²² and negatively-charged functional groups.²³ Chieng and co-workers have reported on the structure and morphology of microporous materials prepared by microemulsion polymerization of mostly methacrylates.^{24–26} However, the relationship between the polymer property and the imprinted droplet size is not clear, and many aspects of such materials remain to be investigated.

In an effort to study the relationship between the size of the imprinted cavities in such polymer resins and the water contents in the reverse micelles, we have prepared a series of polymers imprinted with reverse micelles containing varying amounts of water. The surface area, pore volume, pore size, and size distribution of these polymers have been measured by the Brunauer–Emmett–Teller (BET) gas adsorption experiments. We report here the preparation and characterization of the polymer resins with cavities of different sizes and size distributions.

Experimental Section

Styrene (S) and divinylbenzene (DVB) were purchased from Aldrich, washed with aqueous NaOH, and redistilled before use. The cross-linker DVB is 55% pure, and the redistillation did not change its apparent composition. Sodium bis(2-ethylhexyl) sulfosuccinate (AOT) was purchased from Sigma and used as received. The free radical initiator, 2,2'-azobisisobutyronitrile (AIBN), purchased from Eastman Kodak, was recrystallized prior to use. The solvents for extraction and washing were used as received.

The preparation of the polymer resins is shown schematically in Figure 1. Studies have been carried out to obtain optimal chemical compositions and preparation conditions of the polymers. The polymer resins in this report were prepared with the concentration of AOT fixed at 0.2 M in the mixture

* To whom correspondence should be addressed. Tel: (514) 343-7633. Fax: (514) 343-7586. E-mail: zhuj@ere.umontreal.ca.

[®] Abstract published in *Advance ACS Abstracts*, May 1, 1997.

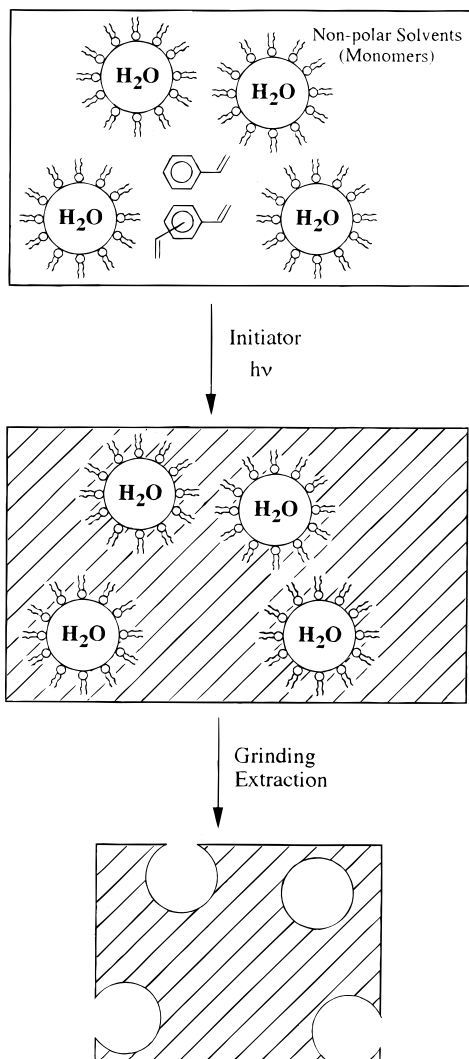


Figure 1. Preparation scheme of the polymer resins. The pore size can be controlled by adjusting the water content inside the reverse micelles prior to polymerization.

of monomers. With the help of minute amounts of water, AOT can readily dissolve in nonpolar solvents, in this case a mixture of styrene and divinylbenzene. DVB (which contained impurities such as ethylvinylbenzenes) was 20–50 vol % of the monomer mixtures with styrene. Typically, after dissolving the appropriate amount of AOT in the monomer mixture, deionized water was then added to the system to adjust the water-to-AOT molar ratio (W) from 1 to 18, beyond which the solution was no longer homogeneous. The formation and good dispersion of the reverse micelles were ensured by sonification in an ultrasonic bath. Bulk polymerization took place upon the addition of 2 wt % of AIBN and ultraviolet (UV) irradiation at a wavelength of 254 nm in a UV cross-linker (UVC-515 UV Multilinker, Ultra-Lum, Carson, CA) over a period of 6–12 h, depending on the quantity of the sample. During the polymerization, no attempt was made to control the temperature of the samples. It was found that the temperature increased slightly after prolonged irradiation under UV light. The polymers obtained were ground with a micromill (Bel-Art, Pequannock, NJ) equipped with cold-water cooling system and then washed with toluene, ethanol, and ether successively in a Soxhlet extractor. They were dried and sieved before characterization.

The BET gas adsorption measurements were performed on a Coulter SA-3100 surface area and pore size analyzer (Coulter Scientific, Miami, FL) with nitrogen to determine the surface area, pore volume and size, and size distribution of the polymer resins. Helium was used to determine the free space in the sample cell. Polymer resins with mesh size between 60 and 100 (150–250 μm) were normally used for the measurements

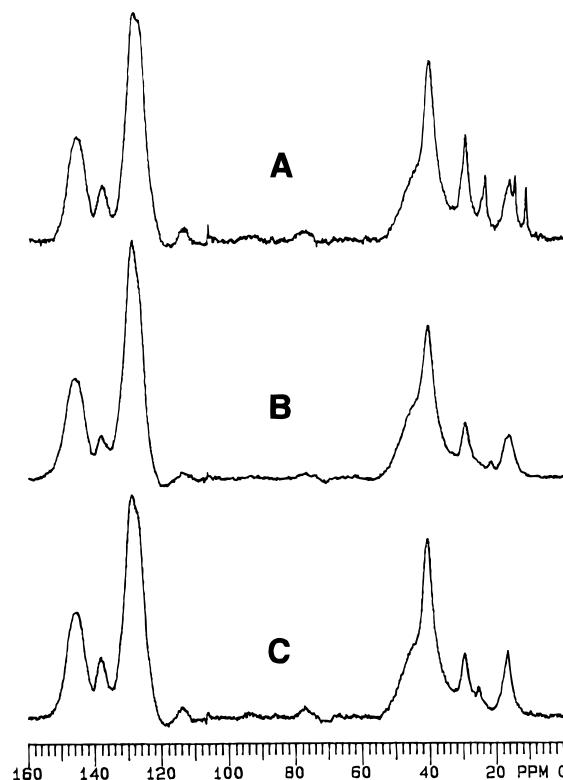


Figure 2. Solid state CP/MAS ^{13}C NMR spectra of polymer resins showing the effectiveness of the Soxhlet extraction: (A) a polymer resin (S:DVB = 4:1 (v/v), [AOT] = 0.2 M, $W = 12$) before extraction; (B) the same polymer after extraction, showing the disappearance of AOT peaks from 10 to 35 ppm, which is approximately identical to (C) a poly(styrene-*co*-divinylbenzene) resin (S:DVB = 4:1) prepared by the same method without AOT.

unless otherwise specified. The pore size distribution reported here was obtained from the desorption isotherm by the use of the Barrett–Joyner–Halender (BJH) method.²⁷ The solid state cross polarization magic angle spinning (CP/MAS) NMR spectra were recorded at room temperature on a Varian VXR-300 NMR spectrometer equipped with a Doty CP/MAS probe operating at 75 MHz for ^{13}C and a spinning rate at ca. 4 kHz. The contact time (1.5 ms), relaxation delay (5 s), and other parameters were optimized for the comparison of the ^{13}C CP/MAS NMR spectra.

Results and Discussion

Solid State NMR Spectroscopy. As shown in the solid state ^{13}C CP/MAS NMR spectra of the polymer resins (Figure 2), the intensities of the ^{13}C NMR signals due to the aliphatic chains of the surfactant AOT (10–35 ppm) are much diminished after washing. The NMR signals of AOT can be identified easily by comparison of the spectrum for the polymer resin containing AOT (Figure 2A) with that of the same polymer after washing (Figure 2B) or that of a polymer made without any surfactant (Figure 2C). In fact the NMR spectrum of the polymer resin after washing (Figure 2B) is very similar to that of a polymer resin prepared without AOT reverse micelles (Figure 2C). The NMR spectra show that most AOT molecules have been successfully extracted from the ground polymer resins. It is still possible, however, that residual AOT molecules were trapped in the unexposed pores inside the polymer matrix even after grinding and extensive washing. The remaining surfactants, if any, should not affect the use of the polymers because of the heavy cross-linking.

BET Surface Area and Pore Volume Measurements. The BET gas adsorption experiments were used

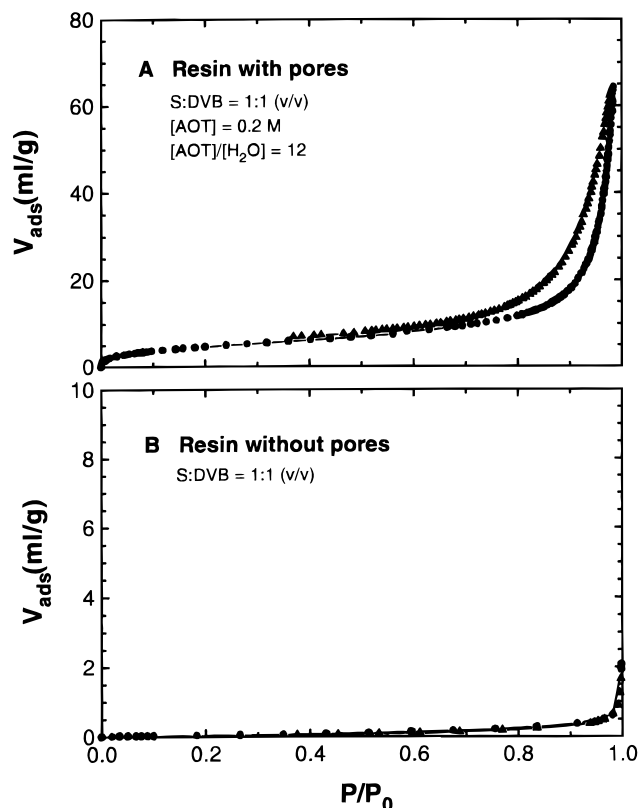


Figure 3. Gas adsorption-desorption hysteresis loops of two polymer resins (volume of gas adsorbed as a function of relative pressure): (A) a polymer resin with pores created by AOT reverse micelles (S:DVB = 1:1 (v/v), [AOT] = 0.2 M, $W = 12$); (B) a polymer resin made from styrene-divinylbenzene prepared with the same procedure in the absence of AOT reverse micelles (S:DVB = 1:1 (v/v), no AOT, no water). The circles and triangles represent the adsorption and desorption isotherms, respectively. Note that the presence of pores in the material is clearly shown by the quantity of gas adsorbed and by the difference between the adsorption and desorption isotherms.

to determine important physical parameters such as the surface area, the pore volume, the cavity size, and the distribution of the cavity sizes.²⁸ The adsorption-desorption hysteresis loops of two typical polymer resins are shown in Figure 3. When the material is porous, the adsorption and desorption isotherms do not overlay on each other because of the porous structure of the material (Figure 3A). On the other hand, for a nonporous material, the amount of gas adsorbed is small and no significant difference of the two isotherms can be observed (Figure 3B). In addition, the volume of gas adsorbed on a nonporous material is very low (Figure 3B) when compared with a porous one (Figure 3A).

From the hysteresis loops shown in Figure 3 the pore size distribution can be calculated by the use of the BJH method. Figure 4 shows the pore size distribution curves of two polymer resins calculated from the desorption isotherms. The two resins were designed to possess pores of different sizes by the adjustment of the amount of water solubilized in the reverse micelles prior to the polymerization. The maxima of the two distribution curves indicate the respective pore size at which there is a largest pore volume increment. Clearly, the pore size inside the polymers can be controlled by adjusting the water-to-AOT molar ratio (W) in the reverse micelles. When W is changed from 1 to 14 at ca. 40 vol % cross-linking (i.e., S:DVB = 3:2), the pore size with the maximum pore volume increased from 7.5 to 36 nm.

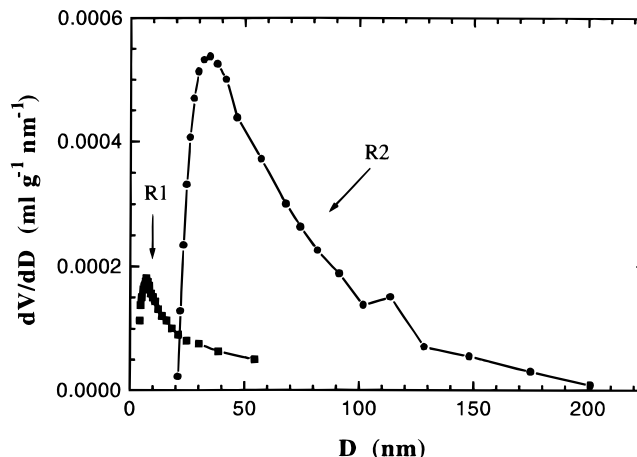


Figure 4. Distribution of pore diameters of two polymer resins with different pore sizes, as determined by the BET method. In the figure, the derivative of the pore volume (dV/dD) is shown as a function of pore diameter (D). Both resins, [AOT] = 0.2 M, S:DVB = 3:2 (v/v). R1, $W = 1$; R2, $W = 14$. Note that the integration of the area beneath the distribution curve gives the total pore volume of the material per unit weight (gram).

It is of importance to note that the degree of cross-linking of the polymer resins has an effect on the pore size in the polymer resins. In this report, we use the volume ratio of S to DVB, where the DVB sample is only 55% pure and contained impurities such as ethylvinylbenzenes. The real degree of cross-linking should be much lower. If we assume the impurities had the same density as DVB, the degree of cross-linking of the resins could be better described as about 55% of the volume fraction of DVB as appeared in this report.

Figure 4 also shows that the pore size distribution is significantly narrower for the polymer resin prepared with lower W in the reverse micelles. This means that when the water content in the micelles is low, the size of the micelles is small but much more uniform. This is consistent with the observation of an increased polydispersity of the micellar size with increasing water content.²⁹ As W increases, the size of the micelles increases but becomes less uniform, which is an indication of increased dynamic movements of the micelles in the monomer solutions. It may be possible, therefore, to narrow this distribution by changing the AOT concentration and by ensuring a good dispersion of the micelles.

The integration of the area under the distribution curve provides a comparison of the total pore volume in a unit weight of the respective polymer resins. Figure 4 gives clear indications of the dependence of both pore size and total pore volume on the water content in the reverse micelles. The total pore volume in the polymers increased with increasing average pore sizes.

The BET gas adsorption experiments provided a direct correlation between the size of the imprinting templates (the reverse micelles) and the size of the microcavities formed in the polymer resins. Such a correlation is shown in Figure 5. It is known in the literature that the size of the reverse micelles increases more or less linearly as a function of water content in the micelles. Three of the proposed linear relationships for the reverse micelles³⁰⁻³² are shown in Figure 5. These reproduced lines are similar and almost parallel to each other. The differences in the lines may be a result of the different nonpolar solvents used in the preparation of the AOT reverse micelles, or due to the

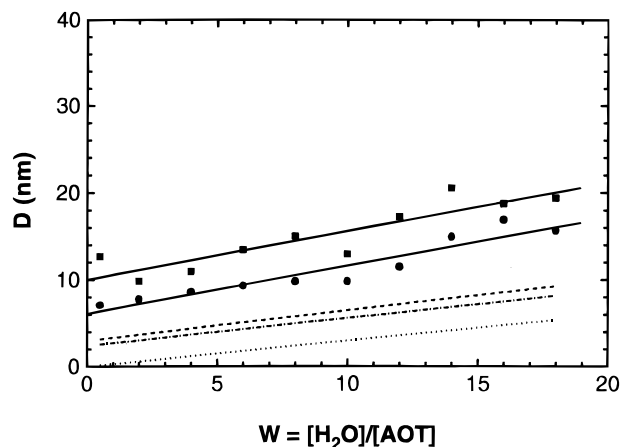


Figure 5. Change of the average pore diameter (D_{av}), the diameter of pores with the maximum pore volume (D_{mv}) of the polymer resins, and the reverse micellar size as a function of the water content W : squares, D_{av} ; circles, D_{mv} . Solid lines are linear regressions of D_{av} and D_{mv} . Lines of dashes, dash-dots, and dots are reproduced from refs 29, 30, and 31, respectively.

experimental differences. In our case, the nonpolar solvent is a S-DVB mixture. The instability of the monomers would make such studies difficult if not impossible. However, it is interesting to note that the pore sizes in the polymer resins also vary in a linear fashion as a function of water content W in the original reverse micelles. Both the average pore diameter (D_{av}) and the diameter of pores with maximum volume (D_{mv}) as a function of W are shown in Figure 5. In general a linear relationship between the diameters and W can be found. Linear regression provides the following relationships

$$D_{av} = 0.56W + 9.8 \quad (1)$$

and

$$D_{mv} = 0.55W + 6.1 \quad (2)$$

where the unit of D_{av} and D_{mv} is given in nanometers. It should be noted that the relationships in eqs 1 and 2 are valid for this particular series of polymers. The diameter of the pores also varies as a function of the degree of cross-linking as well as the concentration of surfactants.

Because of the asymmetric nature of the distribution curves (Figure 4), the average pore diameter D_{av} is higher than the values of D_{mv} . The D_{mv} values represent the maxima of the distribution curves and can be determined with a greater precision. However, as seen in Figure 5, the errors in the D_{av} values are relatively larger, which is caused also by the asymmetry of the distribution curves. Both D_{av} and D_{mv} are larger than the sizes of the original reverse micelles. The removal of the surfactants from the cavities imprinted with the reverse micelles would also lead to an increase in the pore size of the polymer resins as compared to the size of the reverse micelles. It is evident that the pore sizes in the polymer resins can be controlled by adjusting the water content in the reverse micelles of AOT prior to the polymerization process.

Figure 6 shows the changes of the specific surface area and pore volume as a function of W . The surface area and total pore volume in the polymer resin were both found to increase more or less linearly with increasing W at the beginning up to a certain point after which they leveled off (Figure 6). The surface area and

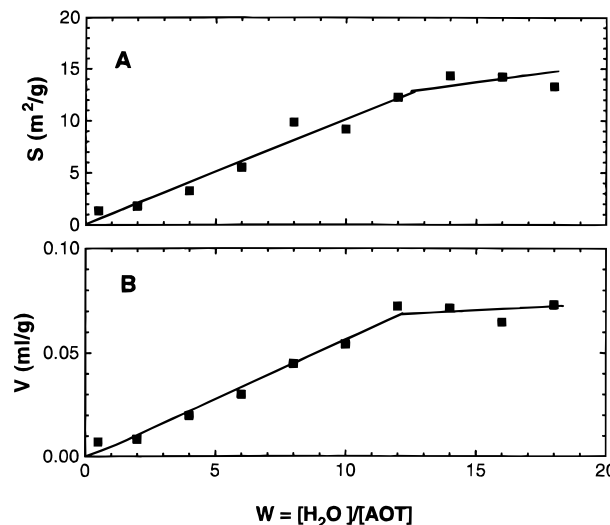


Figure 6. Specific surface area (A) and total pore volume (B) plotted as a function of water content in the reverse micelles. Samples with varying W : S:DVB = 1:1 (v/v), [AOT] = 0.2 M.

Table 1. Effect of Resin Particle Size on Certain Physical Parameters^a

particle size range		surface area (m ² /g)	pore volume (mL/g)	pore diameter <i>D</i> _{mv} (nm)
mesh size (US standard)	diameter (μm)			
<100	<150	15.81	0.0903	11.68
60–100	150–250	13.32	0.0742	11.95
40–60	250–425	12.98	0.0672	11.30

^a Polymer resin: S:DVB = 1:1 (v/v); [AOT] = 0.2 M; $W = [H_2O]/[AOT] = 12$.

pore volume are both functions of the number of pores and the size of the pores. At a given AOT concentration, large pore sizes (caused by large W) beyond a certain point may not necessarily lead to an increase in the specific surface area or total pore volume.

Effect of the Particle Size. Since the particle size can affect the surface area and even the availability of the pores of the resins, the ground polymers were sieved into three different fractions with the following mesh sizes: below 100 (particle diameter <150 μm), between 60 and 100 (150–250 μm), between 40 and 60 (250–425 μm). The surface area, pore volume, and pore size of a polymer resin (S:DVB = 1:1 (v/v), [AOT] = 0.2 M, $W = 12$) ground into different particle sizes were measured with results listed in Table 1. In general, the effect of particle size is not very significant, but surface area and pore volume show increases as the particle size decreases. Smaller particles in a unit weight of solid sample have larger surface areas, and finer grinding can make more pores exposed and available. As shown in the table, the characteristic pore diameter, however, remains unchanged.

Thermal Stability. It is well-known that polystyrene is a stable polymer over a large temperature range. Its glass transition temperature (T_g) is in the range of 85–100 °C, depending on the molecular weight, and its melting temperature is about 250 °C.³³ It is known that an increase in molecular weight or cross-linking usually leads to an increased T_g . No obvious T_g was detected for such highly cross-linked polymers. Thermal analyses of the samples showed that the polymers were stable up to their decomposition temperature at over 300 °C. The cavity size and shape were found to remain stable for an extended period of time (up to 48 h) at elevated temperatures (up to 120 °C). It was noticed that the

polymers became more resistant to mechanical crushing (as in grinding) when the degree of cross-linking was high. We have observed that, during the grinding of the samples, the normally brittle materials became difficult to break as the temperature of the sample rose when cooling was not efficient.

Concluding Remarks

We have shown that the control of the pore size and distribution in cross-linked polymer resins can be achieved by the reverse micellar imprinting technique. Polymer resins with a desired cavity size and surface area within a certain range can be made by varying the water content in the reverse micelles prior to polymerization. We have used the styrene-divinylbenzene-based polymers with reverse micellar imprints in this study, though other monomers can also be used. It is known that the microcavities can help to improve the resolution of separation of structurally related chemical compounds.^{6,9,20,21} It would be interesting to study the correlation between the size of the cavities in the polymers and the size and shape of the guest molecules in the chromatographic separations of mixtures of chemical compounds.

Acknowledgment. Financial support from the Environmental Science and Technology Alliance Canada (ESTAC) and the Natural Sciences and Engineering Research Council (NSERC) of Canada is gratefully acknowledged. R.Y. thanks NSERC for a summer studentship.

References and Notes

- (1) Smigol, V.; Svec, F.; Fréchet, J. M. J. *Macromolecules* **1993**, *26*, 5615.
- (2) Zhu, X. X.; Wang, F.; Nivaggioli, T.; Winnik, M. A.; Macdonald, P. M. *Macromolecules* **1993**, *26*, 6397.
- (3) Petit, J.-M.; Zhu, X. X.; Macdonald, P. M. *Macromolecules* **1996**, *29*, 70.
- (4) Shea, K. J.; Sasaki, D. Y. *J. Am. Chem. Soc.* **1989**, *111*, 3442.
- (5) Shea, K. J.; Spivak, D. A.; Sellergren, B. *J. Am. Chem. Soc.* **1993**, *115*, 3368.
- (6) Wulff, G. In *Polymeric Reagents and Catalysts*; Ford, W. T., Ed.; American Chemical Society: Washington, DC, 1986; p 186.
- (7) Sellergren, B.; Lepisto, M.; Mosbach, K. *J. Am. Chem. Soc.* **1988**, *110*, 5853.
- (8) Wulff, G.; Schauhoff, S. *J. Org. Chem.* **1991**, *56*, 395.
- (9) Sellergren, B.; Lepisto, M.; Mosbach, K. *J. Am. Chem. Soc.* **1988**, *110*, 5853.
- (10) Arnold, F. H.; Dhah, P.; Shnek, D.; Plunkett, S. US Patent 91-649470, 1992.
- (11) Dabulis, K.; Klivanov, A. M. *Biotechnol. Bioeng.* **1992**, *39*, 176.
- (12) Viatakis, G.; Andersson, L. I.; Mueller, R.; Mosbach, K. *Nature* **1993**, *361*, 645.
- (13) Damen, J.; Neckers, D. C. *J. Am. Chem. Soc.* **1980**, *102*, 3265.
- (14) Bardez, E.; Monnier, E.; Valeur, B. *J. Phys. Chem.* **1985**, *89*, 5031.
- (15) Jain, T. K.; Varshney, M.; Maitra, A. *J. Phys. Chem.* **1989**, *93*, 7409.
- (16) Bardez, E.; Goguillon, B.-T.; Keh, E.; Valeur, B. *J. Phys. Chem.* **1984**, *88*, 1909.
- (17) Zhu, X. X.; Bardez, E.; Dallery, L.; Larrey, B.; Valeur, B. *New J. Chem.* **1992**, *16*, 973.
- (18) Sasthav, M.; Cheung, H. M. *Langmuir* **1991**, *7*, 1378.
- (19) Raj, W. R. P.; Sasthav, M.; Cheung, H. M. *Langmuir* **1991**, *7*, 2586.
- (20) Menger, F. M.; Tsuno, T.; Hammond, G. S. *J. Am. Chem. Soc.* **1990**, *112*, 1263.
- (21) Menger, F. M.; Tsuno, T. *J. Am. Chem. Soc.* **1990**, *112*, 6723.
- (22) Ruckenstein, E.; Hong, L. *Chem. Mater.* **1992**, *4*, 122.
- (23) Sundell, M. J.; Pajunen, E. O.; Hormi, O. E. O.; Näsman, J. H. *Chem. Mater.* **1993**, *5*, 372.
- (24) Gan, L. M.; Chieng, T. H.; Chew, C. H.; Ng, S. C. *Langmuir* **1994**, *10*, 4022.
- (25) Chieng, T. H.; Gan, L. M.; Chew, C. H.; Ng, S. C. *Polymer* **1995**, *36*, 1941.
- (26) Chieng, T. H.; Gan, L. M.; Chew, C. H.; Ng, S. C.; Pey, K. L. *Langmuir* **1996**, *12*, 319.
- (27) Barrett, E. P.; Joyner, L. G.; Halender, P. H. *J. Am. Chem. Soc.* **1951**, *73*, 373.
- (28) Lowell, S.; Shields, J. E. *Powder Surface Area and Porosity*, 2nd ed.; Chapman and Hall: New York, 1984.
- (29) Zulauf, M.; Eicke, H.-F. *J. Phys. Chem.* **1987**, *91*, 865.
- (30) Pileni, M. P. *J. Phys. Chem.* **1993**, *97*, 6961.
- (31) Kurumada, K.-I.; Shioi, A.; Harada, M. *J. Phys. Chem.* **1994**, *98*, 12382.
- (32) Fletcher, P. D. I.; Howe, A. M.; Robinson, B. H., *J. Chem. Soc., Faraday Trans. 1* **1987**, *83*, 985.
- (33) Sperling, L. H. *Introduction to Physical Polymer Science*, 2nd ed.; Wiley: New York, 1992; p 303.

MA961580G